

Optical switching by capillary condensation

PIERRE BARTHELEMY^{1*}, MHER GHULINYAN², ZENO GABURRO², COSTANZA TONINELLI¹, LORENZO PAVESI² AND DIEDERIK S. WIERSMA¹

¹European Laboratory for Nonlinear Spectroscopy and INFN-BEC, via Nello Carrara 1, 50019 Sesto Fiorentino (Florence), Italy

²Nanoscience Laboratory, Department of Physics, University of Trento, via Sommarive 14, I-38050 Povo (Trento), Italy

*e-mail: barthelemy@lens.unifi.it

Published online: 1 March 2007; doi:10.1038/nphoton.2007.24

Photonic materials, which have optical properties that can be modulated by light, are extremely interesting both for their fundamental properties as well as for their potential in the applications of all-optical signal processing and possibly optical computing¹. Earlier studies have been based on nonlinear photonic crystals, and have required relatively high local light intensities to be used^{2–5}. We propose a completely different strategy based on the interplay between light propagation and capillary condensation of gases in porous photonic structures. We show experimentally that the local light intensity can alter the gas/liquid phase equilibrium inside the pores, which allows the refractive-index distribution inside the material to be optically tuned. As a specific example, we show how this feature can be used to obtain optical bistability in porous superlattices. Our results provide a new approach for achieving optical control in photonic systems.

Modulation of the optical properties of materials using light itself usually relies on the nonlinear properties of materials. The refractive index depends on intensity through nonlinear material coefficients, which are generally very small. Very high intensities are therefore required if one wishes to use regular nonlinear optics to create, for example, all-optical photonic switches. Resonant effects, such as band-edge states of photonic crystals, can increase the local intensity by several orders of magnitude and enhance the efficiency with which the nonlinearity is applied.

Here we report on a phenomenon that allows optical modulation to be obtained at low power density, using the interplay between the condensation of gases in porous photonic materials and the propagation of light. Many photonic materials are porous, including silicon-based photonic crystals fabricated by inverting artificial opals or obtained by etching. This includes one-dimensional superlattices and two-dimensional photonic crystals⁶. We will show that one can obtain all-optical modulation of the photonic structure of such porous materials using capillary condensation. As an example, we demonstrate that this allows optical bistability to be achieved in porous superlattices at relatively low power. However, the results presented have general validity and can be applied also to the more complex two- and three-dimensional silicon structures mentioned above.

Directing a flow of organic vapour close to its saturation point onto a porous medium leads to capillary condensation^{7,8}. Vapour molecules adsorb onto the pore walls and their accumulation

induces the formation of a liquid phase, filling up the pores with dimensions below the critical radius, r_c . In cylindrical pores open at both ends, a modified Kelvin equation⁹ relates r_c to the vapour partial pressure P ,

$$r_c = \frac{v_m \gamma}{k_B T \ln(P_0/P)} \quad (1)$$

where P_0 is the saturation pressure, v_m is the adsorbate molecular volume, γ is the surface tension k_B is Boltzmann's constant and T is the temperature. Substituting partially the air volume fraction, condensation leads to an important modification of the effective refractive index of the porous material ($\Delta n/n \approx 10^{-2}$) (ref. 10).

Optical superlattices can be made from porous silicon with pore sizes in the range of tens of nanometres, close to the critical diameter of vapour condensation at ambient temperatures¹⁰. In the samples prepared specifically for this study (see Methods), the refractive index was modulated periodically and a linear gradient in the refractive index was superimposed on this variation. A superlattice was realized this way, for which the central frequency of the photonic bands depended on position inside the sample. This results in the optical equivalent of Wannier–Stark ladders^{11,12}. At a critical gradient, two modes of the Wannier–Stark ladders can couple resonantly and delocalize through the superlattice. This creates an intense transmission channel, optical analogue of resonant Zener tunnelling (ZT) (ref. 13) (see Supplementary Information, Fig. 1).

Capillary condensation was used to bring these samples in and out of the tunnelling regime (Fig. 1). Flowing an organic vapour on the superlattice, the refractive-index modulation due to capillary condensation modifies the photonic-band structure. Because the pore size depends on depth inside the sample, vapour condensation changes the refractive-index gradient. The critical radius depends on temperature, as shown in equation (1), so local heating induced by light propagating inside the sample results in a modulation of the phase equilibrium in the pores. This introduces an interplay between optical transport and condensation; the laser alters the liquid volume fraction, which modifies the photonic density of states, influencing again light propagation.

We performed transmission measurements in which an incident white-light beam was focused on the superlattice collinearly with a

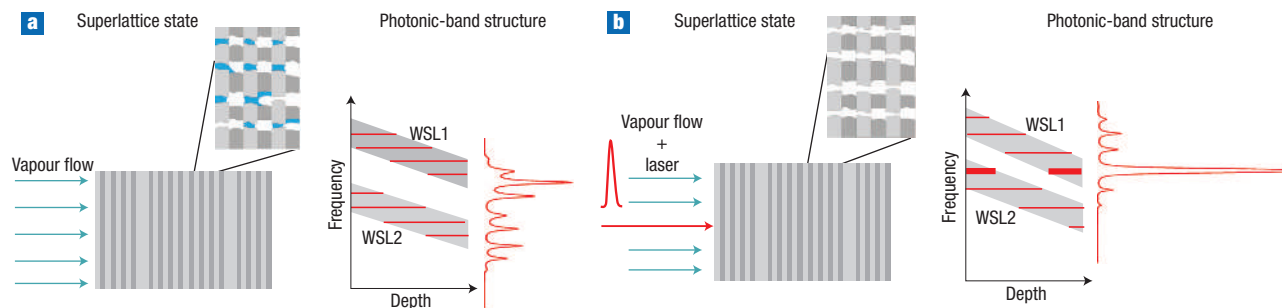


Figure 1 Environment-dependent optical modulation of the photonic-band structure in porous optical superlattices. **a**, Under vapour exposure, capillary condensation induces the formation of a liquid phase in the pores. The resulting refractive-index modification prevents the Wannier–Stark ladders (WSL1 and WSL2) from coupling, leading to low transmission. **b**, Laser-induced evaporation restores the resonant coupling between the Wannier–Stark states and allows a resonant transmission channel to be recovered. Red trace: superlattice transmission spectrum.

laser pump beam. A fibre bunch collected the transmitted signals, which were sent to a spectrometer interfaced to a cooled CCD. A flow of ethanol vapour was realized close to the sample surface using a gas-controller device.

This setup was used in two modes. In the first mode, we realized pump-probe experiments recording the transmitted spectrum of the white-light lamp as a function of pump power (Fig. 2). Vapour exposure shifts the Zener transmission peak towards longer wavelengths and perturbs the coupling between the Wannier–Stark states, thereby broadening and lowering the transmission peak. The local heating induced by the light intensity inside the sample reduces the liquid fraction, and the transmission gradually recovers.

In the second mode, we used a laser with wavelength close to the ZT peak (in this case a laser diode emitting at 973 nm, focused on a spot of 50 μm diameter) and recorded its transmitted power. We exposed a superlattice tuned to ZT at 967 nm. We observed optical bistability^{14,15}, which can be understood as follows (Fig. 3). At low incident power, the laser is poorly coupled with the low-transmission Wannier–Stark states, and the intensity inside the sample is low. Raising the incident power, the liquid fraction decreases and ZT gradually recovers. At a certain power threshold of $P_{\text{th}1} = 12 \text{ mW}$ (corresponding to 600 W cm^{-2}), a cascade occurs, and the intensity inside the sample increases while the Wannier–Stark states go into resonance, which consequently increases evaporation. The system then ‘locks’ into the ZT state. This remains stable on further increasing the intensity.

When the power is lowered below $P_{\text{th}1}$, the ZT condition now persists. The intensity inside the sample remains high owing to the efficient resonance. Hence, if we lower the incident power, the system stays in the high-transmission state, and the transmitted-power curve shows a hysteresis. Below a second threshold $P_{\text{th}2} < P_{\text{th}1}$, the intensity becomes insufficient to prevent recondensation, and the superlattice switches back to the initial state. The width of the hysteresis ($P_{\text{th}1} - P_{\text{th}2} = 0.73P_{\text{th}1}$) shows the high efficiency of this process.

We can model this effect in the following way. We define the filling fraction, f , as the volume fraction of the liquid inside the layers. Although the smallest pores can be nearly completely filled, the larger ones can exhibit partial filling¹⁶. The filling fraction should be interpreted as the average value over one monolayer. The average refractive indices of each of the layers can then be calculated from this volume fraction, using the Bruggeman formula¹⁷. In quasi-static conditions, the absorbed power, P_a , is balanced by a power loss proportional to the

temperature difference between that of the sample, T_s , and the atmosphere, T_0 . Filling-fraction variations are assumed to be proportional to temperature variations.

The response of the system is calculated by an iterative algorithm, starting from an initial filling fraction, f_0 . At each step, using the transfer-matrix formalism, we calculate the absorbed power, to estimate the heat unbalance:

$$\Delta P = P_a - k_B(T_s - T_0) = P_a + C_1(f_i - f_0) \quad (2)$$

We update the filling fraction by adding a term proportional to ΔP ,

$$f_i = f_{i-1} + C_2[P_a + C_1(f_{i-1} - f_0)] \quad (3)$$

We then update the refractive-index profile, and iterate the process until convergence is reached. The parameter C_1 determines the

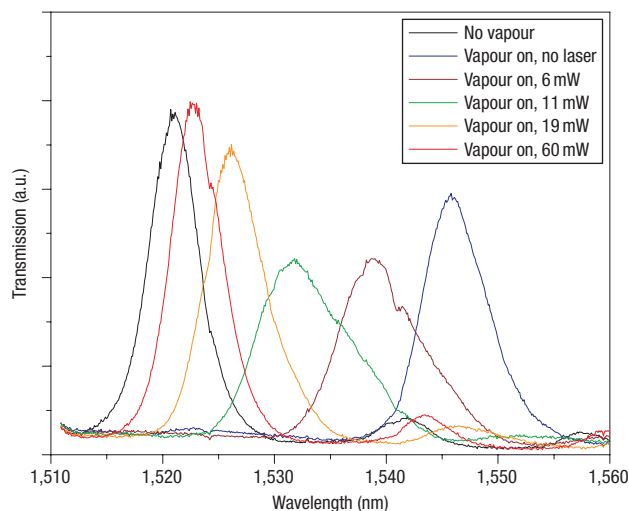


Figure 2 Pump-probe characterization of the vapour-induced optical modulation of porous superlattices. Black line: initial white-light transmission spectrum of the superlattice tuned to ZT. Blue line: vapour exposure redshifts the spectrum and broadens the Zener resonance. Other lines: increasing the pump power (laser wavelength, 810 nm; spot diameter $\approx 200 \mu\text{m}$) allows the Zener resonance wavelength and width to be controlled.

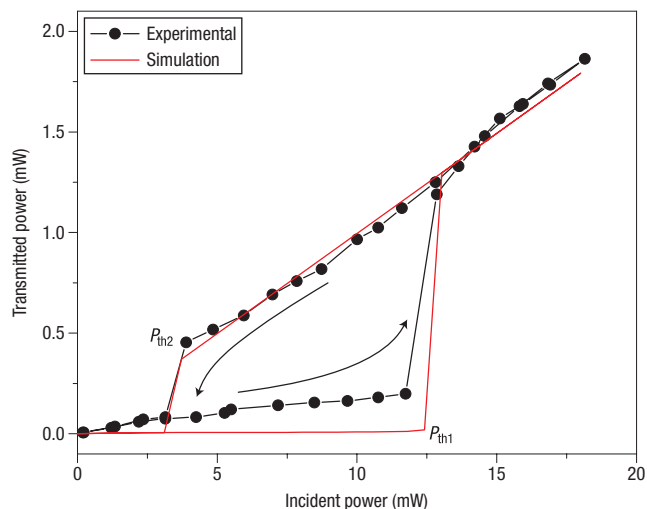


Figure 3 Bistable transmission of a porous optical superlattice exposed to an organic-vapour flow. At low power the incident laser is mainly reflected. At a certain threshold, P_{th1} , the transmitted power increases abruptly. This high-transmission state is stable upon decreasing the incident power. Under a second threshold, P_{th2} , the superlattice switches back to the low-transmission state. Red line: calculated bistable transmission curve. Arrows: evolution direction for increasing/decreasing incident power.

sensitivity of the system. Note that the final result does not depend on C_2 , so this parameter can be adjusted to obtain good convergence velocity.

Our model gives a good insight into the filling-fraction evolution with the incident power. The initial filling fraction has been extracted from experimental spectra, and showed an important variation through the superlattice (from 0.15 to 0.24). Upon raising the incident power, the averaged filling fraction slowly decreased, until the P_{th1} threshold, where an abrupt evaporation occurred (Fig. 4). Decreasing the incident power, the filling fraction stayed low until P_{th2} was reached.

We compared experimental and calculated transmission curves (Fig. 3), adjusting the C_1 parameter in order to superimpose the final state of the high-power transition ($C_1 = 5 \text{ W}^{-1}$). A minimal filling fraction of $f = 0.036$ was introduced in the calculation to obtain a good fit of the high-transmission branch. This corresponds to a residual ethanol fraction that remains unevaporated. The results of this comparison are very satisfying, as the theoretical model recovers, with good accuracy, the hysteresis width and shape, without extra fit parameters.

In conclusion, we have shown how the interplay of gas condensation and light transport in porous photonic systems can lead to optical modulation of the photonic density of states and result, for example, in a bistable transmission at relatively low power density. A simplified model of the quasi-static behaviour is presented, showing a very good agreement with the experiments. The phenomenon provides a new strategy for the development of devices that require optical control, such as all-optical switches. By reducing the device volume, the switching time could be reduced from the current value (~ 10 ms) to the microsecond range¹⁸. The nature of the observed phenomenon also allows potential applications in environment-dependent devices, such as gas sensors and switches depending on humidity and/or partial gas pressure.

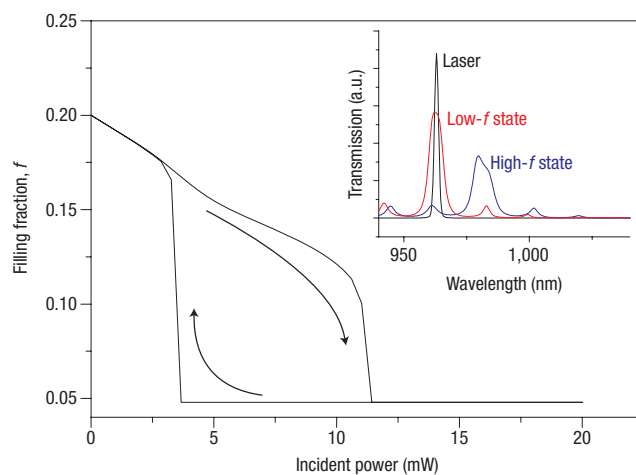


Figure 4 Calculated filling-fraction evolution with the incident laser-power. Increasing the laser power leads to a gradual lowering of the filling fraction. Above a critical power, an abrupt transition of the filling fraction indicates significant evaporation. This evaporated state is stable upon lowering the incident power until a second threshold is reached. (Inset: transmission spectra for the high and low filling fraction conditions). Arrows: evolution direction for increasing/decreasing incident power.

METHODS

Mesoporous optical superlattices were electrochemically etched into boron-doped (100)-oriented silicon substrates with a resistivity of $0.01\text{--}0.02 \Omega \cdot \text{cm}$. Room-temperature anodization was performed using a solution of 30% volumetric fraction of aqueous HF (48 wt%) with ethanol.

The samples consisted of sequences of four different types of layers, A to D, with different porosity and/or thicknesses. Layers A and B were quarter-wave thick layers and had an optical thickness of 260 nm, whereas C and D formed half-wavelength cavities and had optical thicknesses of 426 nm and 499 nm, respectively. C and D cavity layers were alternated with Bragg mirrors formed by alternating A and B. The sample structure corresponded to the sequence BABABCBABABADB ABABABC... (see Supplementary Information, Fig. 1).

Two current densities (50 mA cm^{-2} and 7 mA cm^{-2}) were alternated to etch high- and low-porosity layers. The nominal porosities and the refractive indices were $p_A = p_C = p_D = 68\%$, $n_A = n_C = n_D \approx 1.45$ and $p_B = 50\%$, $n_B \approx 2.1$. Using silicon etch rates (α) for different current densities, the physical thicknesses d of the layers were controlled by the etch duration per layer, defined as $t_{\text{etch}} = d/\alpha$ (see Supplementary Information, Fig. 3). To introduce optical thickness gradients, etch-stop current steps were used, which controlled the resulting refractive index and, therefore, the final optical thickness for each layer. The refractive-index gradients were partially compensated by applying a linear gradient of layer thicknesses (through etch durations). Finally, the samples were made free-standing by applying an electro-polishing current pulse of 0.32 A cm^{-2} at the end of the growth process. The pore size within a monolayer of the superlattice shows a broad distribution (extracted from scanning-electron-microscope analysis), and for the cavity layers ranges from $26 \pm 10 \text{ nm}$ at the low porosity side of the superlattice to $33 \pm 10 \text{ nm}$ at the high porosity side (average monolayer porosity 68% and 76%, respectively).

Received 9 November 2006; accepted 23 January 2007; published 1 March 2007.

References

- Almeida, V. R., Barrios, C. A., Panepucci, R. R. & Lipson, M. All-optical control of light on a silicon chip. *Nature* **431**, 1081–1084 (2004).
- Tan, H. W., van Driel, H. M., Schweizer, S. L., Wehrspohn, R. B. & Gösele, U. Nonlinear optical tuning of a two-dimensional silicon photonic crystal. *Phys. Rev. B* **70**, 205110 (2004).
- Hache, A. & Bourgeois, M. Ultrafast all-optical switching in a silicon based photonic crystal. *Appl. Phys. Lett.* **77**, 4089–4091 (2000).

4. Notomi, M. *et al.* Optical bistable switching action of Si high-Q photonic crystal nanocavities. *Opt. Express* **13**, 2678–2687 (2005).
5. Notomi, M. *et al.* Optical bistable device in one-dimensional photonic crystal waveguide. *Opt. Commun.* **255**, 46–50 (2005).
6. Birner, A., Wehrspohn, R. B., Gösele, U. M. & Busch, K. Silicon-based photonic crystals. *Adv. Mater.* **13**, 377–388 (2001).
7. Evans, R., Marconi, U. M. B. & Tarazona, P. Fluids in narrow pores: Adsorption, capillary condensation, and critical points. *J. Chem. Phys.* **84**, 2376–2399 (1986).
8. Valiullin, R. *et al.* Exploration of molecular dynamics during transient sorption of fluids in mesoporous materials. *Nature* **443**, 965–968 (2006).
9. Thomson, W. On the equilibrium of vapor at a curved surface of liquid. *The London, Edinburgh, Dublin Phil. Mag. J. Sci.* **42**, 448–453 (1871).
10. Ghulinyan, M., Gaburro, Z., Pavesi, L. & Wiersma, D. S. Tuning of resonant Zener tunneling by vapor diffusion and condensation in porous optical superlattice. *Phys. Rev. B* **74**, 045118 (2006).
11. Martijn de Sterke, C., Bright, J. N., Krug, P. A. & Hammon, T. E. Observation of an optical Wannier–Stark ladder. *Phys. Rev. E* **57**, 2365–2370 (1998).
12. Monsivais, G., del Castillo-Mussot, M. & Claro, F. Stark-ladder resonances in the propagation of electromagnetic waves. *Phys. Rev. Lett.* **64**, 1433–1436 (1990).
13. Ghulinyan, M. *et al.* Zener tunneling of light waves in an optical superlattice. *Phys. Rev. Lett.* **94**, 127401 (2005).
14. Gibbs, H. M., McCall, S. L. & Venkatesan, T. N. C. Differential gain and bistability using a sodium-filled Fabry-Perot interferometer. *Phys. Rev. Lett.* **36**, 1135–1138 (1976).
15. Gibbs, H. M. *Optical Bistability: Controlling Light with Light* (Orlando Academic, Orlando, 1985).
16. Kovalev, D. *et al.* Strongly opalescent liquid network formed in a porous silicon matrix. *J. Appl. Phys.* **91**, 4131–4135 (2002).
17. Prinkley, M. T., Lakhtakia, A. & Shanker, B. On the extended Maxwell–Garnett and the extended Bruggeman approaches for dielectric-in-dielectric composites. *Optik* **96**, 25–30 (1994).
18. Vlasov, Y. A., O’Boyle, M., Hamann, H. F. & McNab, S. J. Active control of slow light on a chip with photonic crystal waveguides. *Nature* **438**, 65–69 (2005).

Acknowledgements

We wish to thank P. Bettotti, R. Righini and M. Colocci for discussions, and the entire ‘Optics of Complex Systems’ group at the European Laboratory for Nonlinear Spectroscopy (LENS). The work was financially supported by the Italian Ministry for Education, University and Research through the Cofin 2004 project ‘Silicon-based photonic crystals,’ by the EC (LENS) under contract number RII3-CT-2003-506350, and by the EU through Network of Excellence IST-2-511616-NOE (PHOREMOST). Supplementary information accompanies this paper on www.nature.com/nature photonics Correspondence and requests for materials should be addressed to P.B. (e-mail: barthelemy@lens.unifi.it).

Competing financial interests

The authors declare that they have no competing financial interests

Reprints and permission information is available online at <http://npg.nature.com/reprintsandpermissions/>